We would like to thank the reviewers for their valuable comments and suggestions. We have considered all comments carefully which helped us significantly to improve our manuscript. Following the reviewers' comments and suggestions, we revised the manuscript according to your suggestions. Our responses to the reviewers' comments are listed below in blue fonts and the changes in the manuscript are listed in *blue italic fonts*.

This paper presents a study on the transport of bioaerosols, examining three case studies occurred in March 2020 at Hefei (China). The aerosols are also discriminated into fluorescent and non-fluorescent particles by using a wideband integrated bioaerosols sensor (WIBS) measurements. Also, the biological fluorescent particles are typed into several categories by applying previous methodologies. In combination with a Doppler wind lidar measurements and HYSPLIT back-trajectory modelling their transport is investigated. The relevance of this work can rely on the use of WIBS in-situ instrument in synergy with the Doppler wind lidar (remote sensing) for bioaerosol transport studies, but the novelty of this work is not clearly appreciated.

Therefore, this work could be published, but the following comments should be addressed before it is accepted for publication in AMT.

Thanks a lot for your comments and encouragement. We revised the manuscript according to your comments and suggestion.

General comments:

1. Regarding bioaerosols, although it is mentioned (page 3, lines 73-75), there is no discussion on the potential errors in the WIBS measurements due to the non-biological component of the registered fluorescent particles, whose concentration could be lower than that reported in the paper. Please, include such a discussion.

Thank you for your comment. Additional discussions about the potential errors introduced by fluorescent interferents are added in the revised manuscript.

Changes: line 186-196

"As mentioned before, non-biological fluorescent components on aerosol particles can be fluorescent interferent during WIBS observation. So, the concentrations of fluorescent aerosol particles can be higher than the actual concentration of local fluorescent biological aerosol particles. Proper fluorescent threshold configuration can eliminate these non-biological interferents as much as possible and remain biological particles categorized into fluorescent as many as possible. Although laboratory test (Savage et al., 2017) shows that applying a higher threshold like 6σ or 9σ threshold can effectively exclude interferent like wood smoke and brown carbon from being categorized into fluorescent, filed campaign (Yue et al., 2019) suggest that a proportion of bioaerosols can be misclassified into non-fluorescent particles when elevating

threshold. The 3σ threshold strategy adopted in this paper is to keep consistent with previous works (Crawford et al., 2015; Yu et al., 2016; Yue et al., 2016).”

2. About the type of the bioaerosols more predominantly found in each of the three events examined, it is necessary to provide a more complete explanation in the discussion and justification in the conclusions. Moreover, it must be included a correspondence (maybe in a Table) between each of the WIBS fluorescent particle categories (A, B, C, …, ABC), together with their main fluorescence characteristic/parameters), and their most likely associated type of bioaerosol (fungi, bacteria, pollen, …), in addition to the corresponding, already provided, references. The reading of the paper will indeed be improved.

Thank you for your valuable advice. A table of typical aerosol characterization in WIBS is added as an appendix for reference. And the discussions of possible transported bioaerosol are all improved for a more complete explanation and a more justified conclusion. There are several changes related to the discussion. Parts of them are listed in the following text. Complete changes can be seen in the revised manuscript.

Changes: line 324-344,

“The increased aerosol particles between 3:30–7:30 are more worth noting during this event because they have typical fluorescent characterizations of bioaerosol. As discussed before, the increased aerosol particles during this period contain Type A, Type AB and Type ABC particles, among which the Type AB and Type ABC are dominant, and their decreased Mean D during this period (Fig.2 (d)(g)(j) in the right panel) show that their sizes are mainly distributed in the range of less than 1.5 μm. Previous works (Hernandez et al., 2016; Savage et al., 2017) use WIBS to characterize multiple classes of fluorescent biological aerosol particles and non-biological fluorescent interferent samples in a laboratory setting. A summary of the results of these works is listed in Appendix B for comparison with our works. Detailed information can be found in these references. Compared with laboratory tests, the increased fluorescent aerosol particles have a typical size of bacteria (<1.5 μm) but their fluorescent characterization shows a mixture of Type A, AB, and ABC, which are typical fluorescent types of fungal spores. Pollen fragments are excluded because their typical sizes are much larger and their typical fluorescent types are Type C, BC, and ABC, which is different from that in this event. Some kinds of spore-forming bacteria such as Bacillus subtilis *shows higher fluorescent intensity than other bacteria and are mainly categorized as Type AB particles in a laboratory test (Hernandez et al., 2016) and their larger size multicell aggregates in atmospheric might be categorized as Type ABC because larger fluorescent particles intend to have higher fluorescent intensities (Savage et al., 2017; Yue et al., 2019). Fungal spores can also be found in submicron aerosol particles (Xu et al., 2017), indicating that some of them can have smaller sizes than the laboratory test result. So, it can be inferred from the characterization of increased fluorescent aerosol particles that these transported external bioaerosols are most likely to be bacteria aggregates or fungal spores. Backward trajectory results indicate their sources can be the nearby rural area north of Hefei.”*

Changes: line 404-413

“

The sharp increases of Type FL-1 particles between 6:00–8:30 are worth noting here because they have typical characteristics of bioaerosol. According to the variation of their $Mean\ D$ during this period, the sizes of increased Type FL-1 particles are distributed in the range of 1.3 μm–1.8 μm and their fluorescent types show a mixture of Type A, AB, ABC and a tiny fraction of AC particles. According to previous laboratory tests (Hernandez et al., 2016; Savage et al., 2017) and previous discussion in the 13 March event, these characteristics are similar to that of fungal spores. However, bacteria aggregates cannot be excluded in this event, because in the atmospheric environment, bacteria aggregates can be confused with fungal spores because of their similar sizes and fluorescent spectra (Hernandez et al., 2016) .increased fluorescent particles can both be fungal spores or bacteria aggregates. Backward trajectory result shows that their sources can be the Dabie Mountains in the west of Hefei.

”

Changes: line 468-495

“

Although $F_{Total}\ (Fluor)$ decreases during the transport event, the increasing $F_{Total}\ (A)$ and $F_{Total}\ (AB)$ during the transport event still indicates the potential bioaerosol transport, because bacteria and fungal spores are related with Type FL-1 (usually Type A, AB, ABC particles) particles (Hernandez et al., 2016; Savage et al., 2017). According to their mean diameter, the sizes of these transported Type A and Type AB particles during this event are mainly distributed in the range of larger than 1.8 μm for Type A particles and larger than 2.0 μm for Type AB particles, which means the potential transported bioaerosol particles are the largest among the three transport events. However, it is not appropriate to assume that these increased Type A and Type AB are individual bioaerosol particles. Previous works (Savage et al., 2017; Yue et al., 2019) show that larger fluorescent biological aerosol particles are more likely to exhibit a higher fluorescent intensity and wider fluorescent spectrum range, which means exhibit fluorescent in multiple fluorescent channels in WIBS measurement. For example, larger size fungal spores and pollen have higher probabilities to be categorized as Type ABC particles than smaller bacteria. During this event, the transported external aerosol particles have larger sizes than local aerosol particles, however, the expected particles with the highest fluorescent intensities, Type ABC particles do not show an obvious increase in their fraction to total particles. These phenomena indicate that the larger size transported external fluorescent particles do not have an apparently higher fraction of Type ABC particles, and thus have lower fluorescent efficiency than local fluorescent particles. In addition, considering the transported external Type A and Type AB particles have the particle size and asphericity factor characteristics like mineral dust, it is a better explanation that these transported external large-size Type A and Type AB particles result from the bacteria that attached to dust. Researches reveal that microbial activity is significant in the aerosols from desert regions, even impacting the composition of aerosols in downwind regions (Ho et al., 2005; Hua et al., 2007; Maki

et al., 2014, 2015; Tang et al., 2018). During long-range transport, larger mineral particles attached by bacteria can serve as a shelter and favor the survival of bacteria. Dust-attached bacteria have been found in SEM (scanning electron microscope) images from air samples of previous research (Tang et al., 2018). A field campaign (Maki et al., 2019) in the Gobi Desert, which is the source of this event, reveals that after dust events, bacteria from Bacteroidetes, which are known capable of attaching to coarse particles, increase their relative abundance in air samples. The above results support our explanation of WIBS data.

"

Changes: line 565-566, Appendix B

"

Appendix B

The following table presents typical characterizations of different types of fluorescent biological aerosol particles and potential non-biological fluorescent interferents detected by WIBS. All following results are retrieved from laboratory tests using the old model WIBS-4 instead of WIBS-NEO used in this paper. However, these results should not be treated as absolute "signatures" but references for discrimination between broad bioaerosol categories, due to the differences in instrumental parameters, culture circumstances, and measuring environment. For example, bacteria often exist in the form of multi-cell agglomerates or particle mixtures in the atmospheric environment, exhibiting large sizes than a single cell observed here (Hernandez et al., 2016). Besides, pollens have wider size distribution than fungi due to the fragmentation of larger intact pollen grains, some of which have sizes larger than 10 μm and even beyond the upper limit of WIBS-4 detection (~20 μm) (Hernandez et al., 2016; Savage et al., 2017). And finally, compared with the old WIBS-4, the new model WIBS-NEO maintains the same fluorescence channel configuration but upgrades the data acquisition module of size detection and fluorescence intensity measurement, which may also introduce potential variabilities from these laboratory results.

Table B1. Typical aerosol characterization in WIBS detection

Species	*Diameter*	*AF*	*Most frequent Types in WIBS*	*References*
Bacteria	*<1.5 μm*		*A*	*Hernandez et al., 2016*
Fungal Spores	*2–9 μm*		*A, AB, ABC*	
Pollen (Fragments)	*2–9 μm*		*C, BC, ABC*	
Bacteria: *Bacillus atrophaeus*	*2.2±0.4 μm*	*17.4±4.1*	*A*	*Savage et al., 2017*

Bacteria: *Pseudomonas stutzer*	*1.1±0.3 µm*	*19.2±2.8*	*A*	
Fungal Spores: *Aspergillus brasiliensis*	*3.6±1.8 µm*	*20.8±10.3*	*A, AB*	
Fungal Spores: *Saccharomyces cerevisiae*	*7.2±3.7 µm*	*28.7±16.8*	*AB, ABC, A*	
Pollen Fragment: *Phleum pratense*	*6.0±3.2 µm*	*23.1±13.4*	*A, AB, ABC*	
Pollen Fragment: *Alnus glutinosa*	*6.1±3.2 µm*	*25.2±14.6*	*B, AB, BC, ABC*	
Dust: Gypsum	*4.1±3.0 µm*	*19.3±12.2*	*Non-Fluor*	
HULIS: *Suwannee River fulvic acid standard I*	*1.7±1.0 µm*	*12.0±10.1*	*Non-Fluor, B*	
Brown Carbon: *Glycolaldehyde + methylamine*	*1.2±0.4 µm*	*17.9±24*	*Non-Fluor, B*	
Brown Carbon: *Glyoxal + ammonium sulfate*	*1.3±0.6 µm*	*14.1±3.5*	*A, B, AB*	
Soot: Diesel soot	*1.1±0.4 µm*	*21.2±10.1*	*A*	
Soot: *Wood smoke (Pinus Nigra)*	*1.0±0.7 µm*	*9.5±4.3*	*Non-Fluor, B, AB*	

“

3. Three case studies, occurring all for a short-time period (11-20 March 2020), seem to be a short sampling for the evaluation of bioaerosol transport over Hefei. Please, provide other events (in other seasons, for instance). In particular, the last dust-bioaerosol case should include an extra discussion regarding the relevance of the potential pathogenic biological targets being transported on dust intrusions, for instance, as Hefei (China) is a frequent Asian dust-influenced zone.

Thank you for your valuable suggestions. But unfortunately, we cannot provide more events in this paper. This campaign was only performed in March 2020, during the period the aerosol transport event are rarely captured by lidar, and some suspected events are obscured in lidar observation due to the simultaneous bad weather condition (precipitation and cloudy days often occur in Hefei in Spring). Furthermore, aerosol transport and precipitation can both influence the local bioaerosol. When aerosol transport and precipitation occur at the same time, the variation of WIBS data cannot be attributed to whether aerosol transport or precipitation. These three transport events are presented in the paper because they can be confirmed by the good observation quality in good weather conditions during the time, the difference of wind direction in different altitudes, and the high PM concentration near the ground. Observations using lidar and WIBS in other times and seasons will be performed in the future.

Your suggestion for extra discussion regarding the relevance of the potential pathogenic biological targets being transported on dust intrusions is considered in the revised version. Additional discussion about the dust transport and the resulting health risk is added.

Changes: line 495-500

"The pathogenic bioaerosol during dust transport events is believed to be linked to allergen burden and asthma (Ichinose et al., 2005; Liu et al., 2014), and even multiple diseases such as Kawasaki disease in humans (Rodó et al., 2011) and rust diseases in plants (Fröhlich-Nowoisky et al., 2016). Dust transport events generally occur during spring in Hefei. The WIBS data during this event indicates that the long-range dust transport during spring has potential risks to human health in the Hefei area."

4. Unfortunately, the WIBS instrument only register particles with sizes > 0.5 microns (> 0.8 microns as discussed in the paper). This fact should be highlighted in the paper, as WIBS measurements only can register mostly coarse bioaerosols, missing the contribution of smaller-sized bio-particles.

Thank you for your suggestion. Additional discussion about the limit of WIBS is added in the revised version.

Changes: Page 3, line 78-82

"However, WIBS still has some limitations in detecting bioaerosols. For example, WIBS cannot detect particles whose size is smaller than 0.5 μm, so WIBS has limited potential in the detection of small size bio-particles like viruses and focuses on relatively coarse bioaerosols. Besides, non-biological fluorescent components on aerosol particles, such as polycyclic aromatic hydrocarbons (PAHs), humic acids, and fulvic acids may act as interferent during WIBS measurements."

Other comments:

1. Page 2, line 29: Not only 'fine solid particles', but also coarse solid particles. Please, remove 'fine'.

Corrected as suggested.

Changes: line 31

"Aerosols are suspensions of solid particles or liquid droplets in the atmosphere "

2. Page 4, Section 2.1: Does the wind direction at an angle of 0º corresponds to winds from the North? Does it increase clockwise or opposite? Please, indicate it.

Thank you for your question. Yes, the wind direction at 0° corresponds to winds from the north and increase clockwise. Additional description is added.

Changes: line 134-135

"In this paper, the wind direction of 0° corresponds to horizontal wind from the north, and the angle increases clockwise."

3. Pages 4-7 (Section 2): Please, provide the distance between the diverse instrumentation used. This can give a perspective for potential discrepancies due to the different atmospheric samplings of both the in-situ and remote sensing measurements are carried out.

Thank you for your suggestion. All instruments except the PM monitoring instruments are located on the campus of the University of Science and Technology of China (USTC, 31.84 °N,117.26 °E). Lidar system is located about 100 m west of the building of the School of Earth and Space Science. WIBS and other meteorological instruments are located in the building of the School of Earth and Space Science building. WIBS are located in a room on the top floor of the building and other instruments are on the rooftop of the building. The distance among these in-situ measurement instruments is less than 30 m. The PM monitoring stations are spread all over Hefei, the nearest

station from our lidar is about 2.7 km northwest of the campus. The information about the locations is added in the revised version.

Changes: line 128-131

"The lidar observation is performed on the campus of the University of Science and Technology of China (USTC, 31.84 °N,117.26 °E) located in the urban area of Hefei, Anhui Province. The lidar system is placed on the grassland about 100 m west away from the building of the School of Earth and Space Science (SESS)."

Changes: line 152-158

"During the observation in Hefei, hourly PM concentration data published by the Department of Ecology and Environment of Anhui Province (https://sthjt.ah.gov.cn/) are used to be compared with the lidar observation and surface aerosol concentration measured by WIBS. These data are comprehensive values from the measurement results of multiple stations in Hefei, whose locations are shown in https://aqicn.org/city/hefei/. The nearest station to our lidar is located on Changjiang Middle Road (31.852 °N, 117.25 °E), about 2.7 km northwest of the USTC campus."

Changes: line 161-162

"These instruments are located on the rooftop of the SESS building."

Changes: line 217-218

"During observation, a WIBS instrument (NEO model) is located in a room on the top floor of the SESS building. within 30 m away from those meteorological instruments mentioned before."

4. Page 8, lines 200-203: Please, give the position where the measurements are performed with respect to Hefei.

Thank you for your suggestion. The measurements are performed in the USTC campus (31.84 °N,117.26 °E) located in the urban area of Hefei, about 3 km southwest of the city center. The information is added in the revised version.

Changes: line 128-129

"The lidar observation is performed on the campus of the University of Science and Technology of China (USTC, 31.84 °N,117.26 °E) located in the urban area of Hefei, Anhui Province."

5. Page 8, lines 211-214: Please, justify extensively this statement.

Thank you for your suggestion. The statement here is justified for a more cautious explanation.

Changes: line 249-261

"When the cloud layer stays at the low-altitude layer between 9:00 and 21:00, local weather conditions (Fig. 1(i)) show high humidity (78 %–89 %) and low temperatures (6 ℃–13 ℃), which inhibit aerosol diffusion but favor the accumulation of local aerosols and hygroscopic growth of particles. As such, the increase in particulate matter concentration from 7:00 to 9:00 is mainly attributed to external aerosol transport. The different trend between $PM_{2.5}$ and PM_{10} concentrations after 10:00 can be attributed to their different removal efficiency: large particles have higher hygroscopic growth factors (Haenel et al., 1978; Hänel, 1976), their sizes increase largely through hygroscopic growth, and thus they have a higher probability to be removed by gravitational settlement than smaller particles. As for $PM_{2.5}$, they have lower removal efficiency and their concentration can continue to increase through the intensifying local anthropogenic aerosol emission after morning and the inhibited aerosol diffusion. During the period, $PM_{2.5}$ is observed to exceed the PM_{10} concentration at one time, which can be attributed to the difference between instruments and methods for monitoring $PM_{2.5}$ and PM_{10}."

6. Page 8, lines 220-221: '… due to the difference in observation location …', please, add the distance each other.

Thank you for your suggestion. The distance between WIBS and the nearest PM monitoring station is about 2.7 km. The distance is added in the revised version.

Changes: line 267-270

"The different behavior of PM data and WIBS data may be due to the difference in observation location and monitoring method (As mentioned in Sec.2.2., the nearest PM monitoring location is about 2.7 km northwest of the USTC campus)."

7. Page 10, lines 276-277: Any reference or explanation is needed to justify this sentence.

Thank you for your suggestion. Additional explanations and references are added in the revised version.

Changes: line 351-356

"In previous works, a fall velocity greater than 1 m s^{-1} can be identified as precipitation (Manninen et al., 2018; Wang et al., 2019a) and Doppler spectral will be broadened during precipitation due to additional signal peaks from raindrops (Wei et al., 2021). Although these characteristics are the same as a precipitation event, no rainfall is recorded on the ground during this event (Fig.4(j)).

These observations indicate a virga event, during which the hydrometeors beneath the cloud layer enhance lidar backscatter and evaporate before reaching the ground."

8. Page 13 lines 363-366: A more complete justification/explanation is required for this statement.

Thank you for your suggestion. The context here is totally modified. We abolished the previous explanation that the different ratio of $(N_A + N_{AB})/N_{BC}$ between local and external aerosols are attributed to the survival mechanism of bioaerosol by attaching to other particles. The highly oxygenated HULIS related to Type BC particles have sources including primary emission mechanism and secondary formation. In addition to the previous-mentioned transformation from bioaerosol by photo-oxidation, the abundant air pollution of strong oxidation capacity in urban areas like NO_x and O_3 can contribute to the formation of highly-oxygenated organic aerosol like HULIS. However, in desert areas, these air pollutants are less abundant, which means the main generation mechanism of HULIS can be different between local aerosol and external aerosol. And this can explain the higher concentration and fraction of local Type BC aerosols than external aerosols during observation and its decrease of concentration and fraction during external aerosol transport.

Changes: line 501-516

"

In addition, the abnormal decrease in the concentration of Type BC particles should also be noted during this event. Laboratory test (Hernandez et al., 2016) shows that Type BC particles are not a typical fluorescent type for bacteria and fungal spores. Bacteria and fungal spores are mainly connected with Type FL-1 particles. On contrary, EEM (excitation-emission matrix) analysis result from sampled aerosol (Chen et al., 2016, 2020; Wen et al., 2021; Yue et al., 2019) shows that highly-oxygenated HULIS (humic-like substances) has a similar fluorescent fingerprint to Type BC particles and can thus be non-biological fluorescent interferent during WIBS measurement by categorized into Type BC particles. This point is supported in an Mt. Tai field campaign (Yue et al., 2019) by the moderate correlation between Type BC particles and highly-oxygenated HULIS. Atmospheric HULIS has many sources including primary emission mechanisms like biomass burning, and multiple secondary formation processes (Wu et al., 2021). Compared with rural areas, there are abundant air pollutants of strong oxidation capacity in urban areas like NOx and O3, which may contribute to the formation of highly-oxygenated organic aerosol like HULIS (Tong et al., 2019). This can explain the high concentration and fraction of local Type BC particles and the abnormal decrease of its concentration and fraction during external aerosol transport. This explanation is adopted by previous research (Wen et al., 2021), where they also find the decrease of highly-oxygenated HULIS concentration in the urban area during the dust period."

9. Page 15, line 405: Please, change ‘ground-based-lidar’ by ‘ground-based wind lidar’.

Thank you for your suggestion, the word here is changed to a more formal name ‘ground-based coherent Doppler wind lidar’

Changes: line 539-541

“The combination of UV-LIF based online measurement instruments and ground-based coherent Doppler wind lidar expands the aerosol monitoring parameters and proves to be a potential method for real-time monitoring of fluorescent biological aerosol transport events.”

10. Page 20, Figure 1 (f): Please, use the same vertical scale for PM2.5 and PM10.

Corrected as suggested.

Changes: line 781-788 Figure 1

“

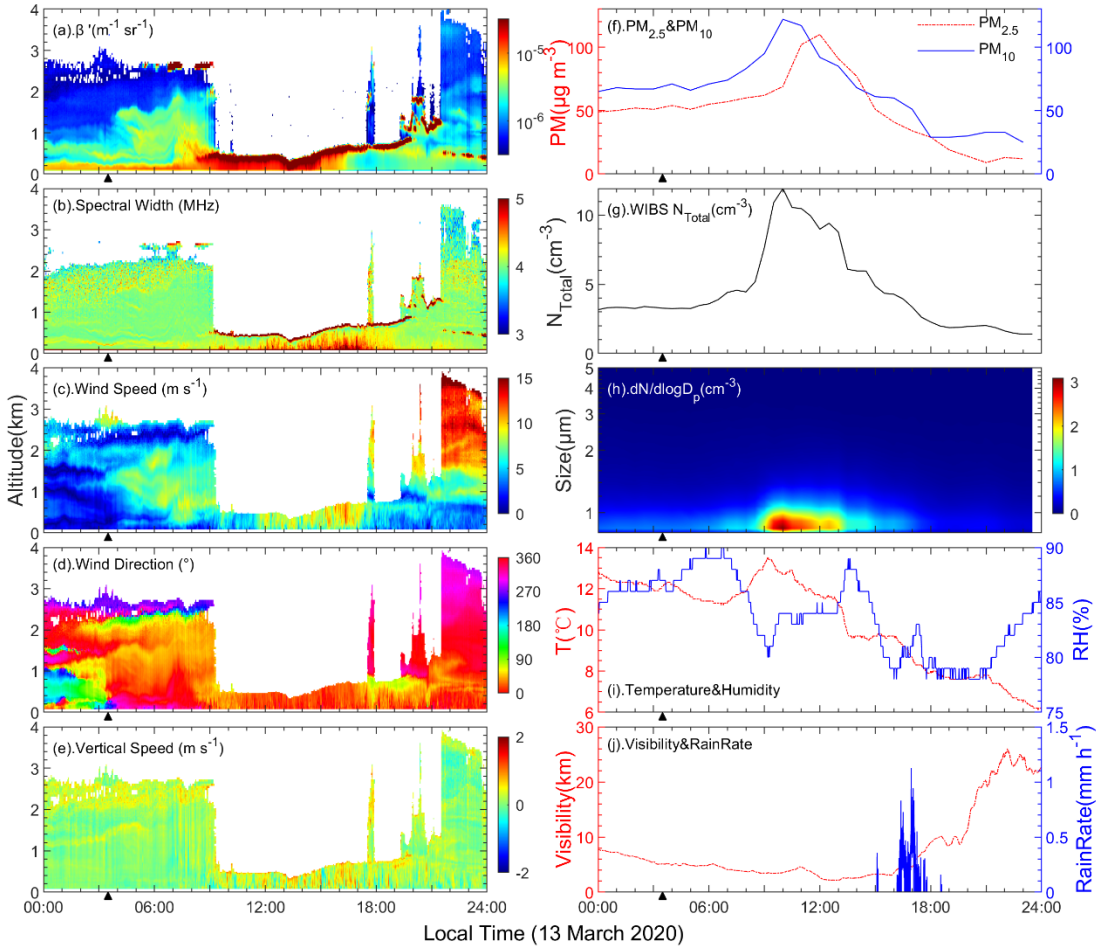

Fig. 1 Left panel: Time-height crosssection of (a) attenuated backscatter coefficient, (b) Doppler spectral width, (c) horizontal wind speed, (d) horizontal wind direction, and (e) vertical wind speed over Hefei observed by CDWL on 13 March 2020. Right panel: simultaneous ground observation results, including (f) surface hourly particulate matter concentration from local monitor network, (g) number concentration and (h) size distribution of surface total aerosol particles from WIBS, (i) local temperature and humidity, and (j) local visibility and rain rate. The wind direction near the surface changes at about 03:30 and is marked with a triangle symbol.

”

11. Page 21, Figure 2 (a)-(j)-right panels: As far as possible, use the same vertical scale for Mean D and Mean AF.

Corrected as suggested.

Changes: line 789-794 Figure 2

“

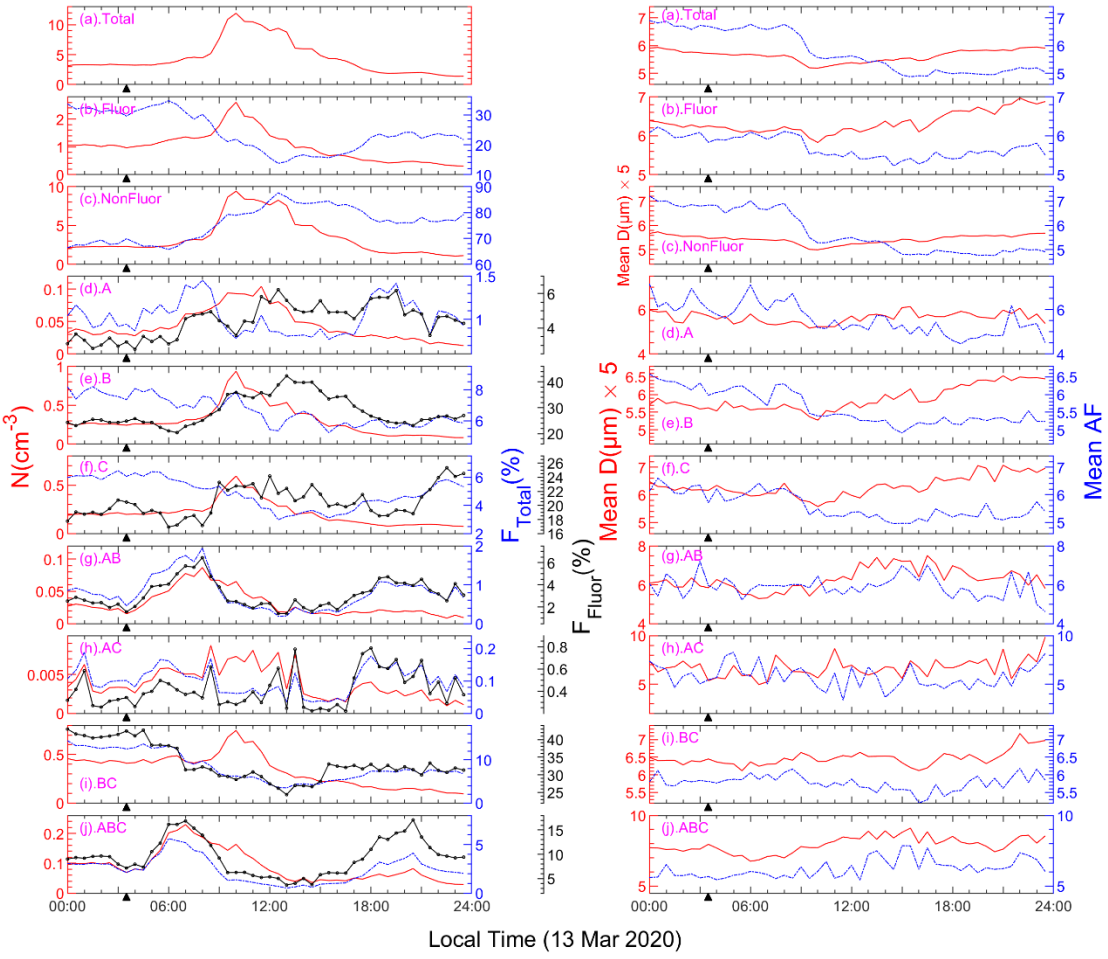

Fig. 2 Left panel: number concentrations (solid red line), number fractions to total particles (blue chain line), and number fractions to fluorescent particles (black solid line with point marker) of the investigated particle types. Right panel: Count mean particle diameter (×5, solid red line) and count mean asphericity factor (blue chain line) of investigated particles measured by WIBS on 13 March 2020. The direction of the wind near the surface changes at about 03:30 and is marked with a triangle symbol.

”

12. Page 23, Figure 4 (f): Please, use the same vertical scale for PM2.5 and PM10.

Corrected as suggested.

Changes: line 801-808 Figure 4

“

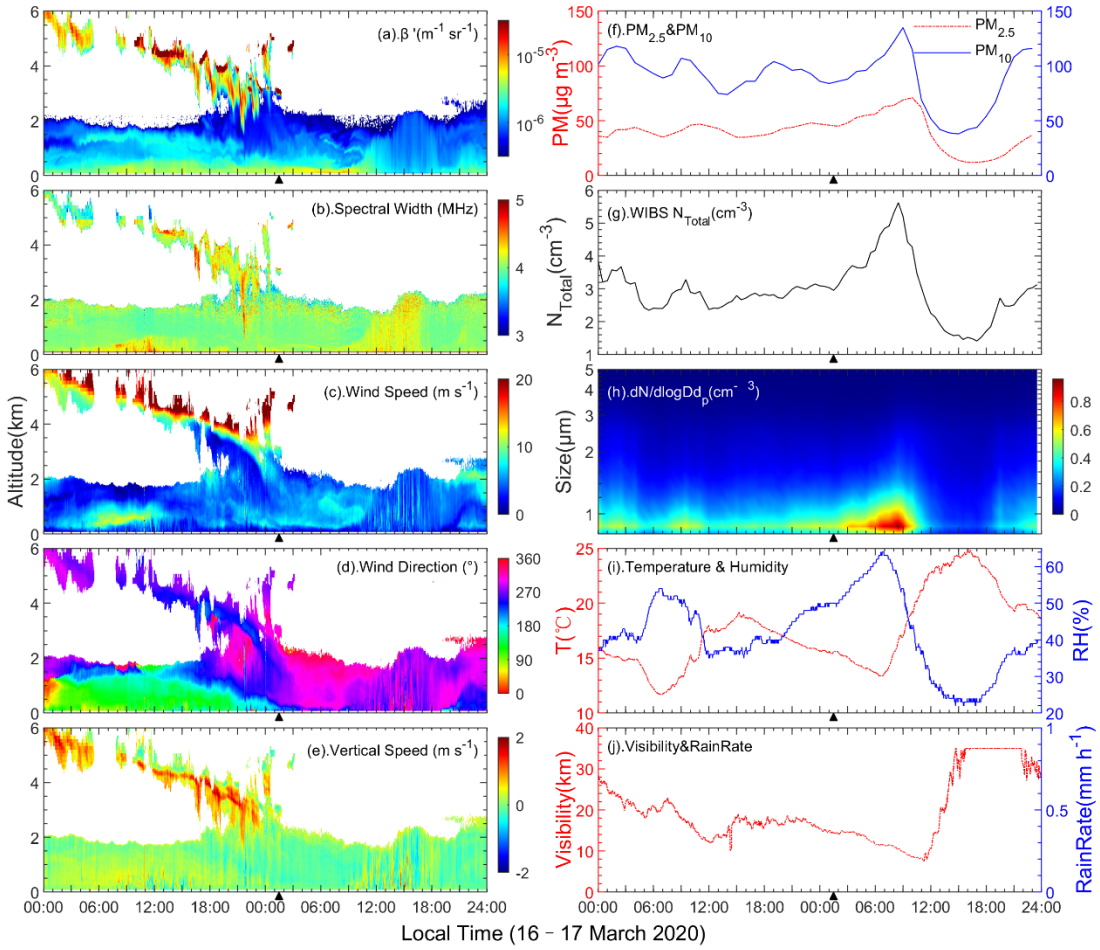

Fig. 4 Left panel: Time-height crosssection of (a) attenuated backscatter coefficient, (b) Doppler spectral width, (c) horizontal wind speed, (d) horizontal wind direction, and (e) vertical wind speed

over Hefei observed by CDWL between 16–17 March 2020. Right panel: simultaneous ground observation results, including (f) surface hourly particulate matter concentration from local monitor network, (g) number concentration and (h) size distribution of surface total aerosol particles from WIBS, (i) local temperature and humidity, and (j) local visibility and rain rate. The wind direction near the surface changes at about 01:30 on 17 March and is marked with a triangle symbol.

"

13. Page 24, Figure 5 (a)-(j)-right panels: As far as possible, use the same vertical scale for Mean D and Mean AF.

Corrected as suggested.

Changes: line 809-814 Figure 5

"

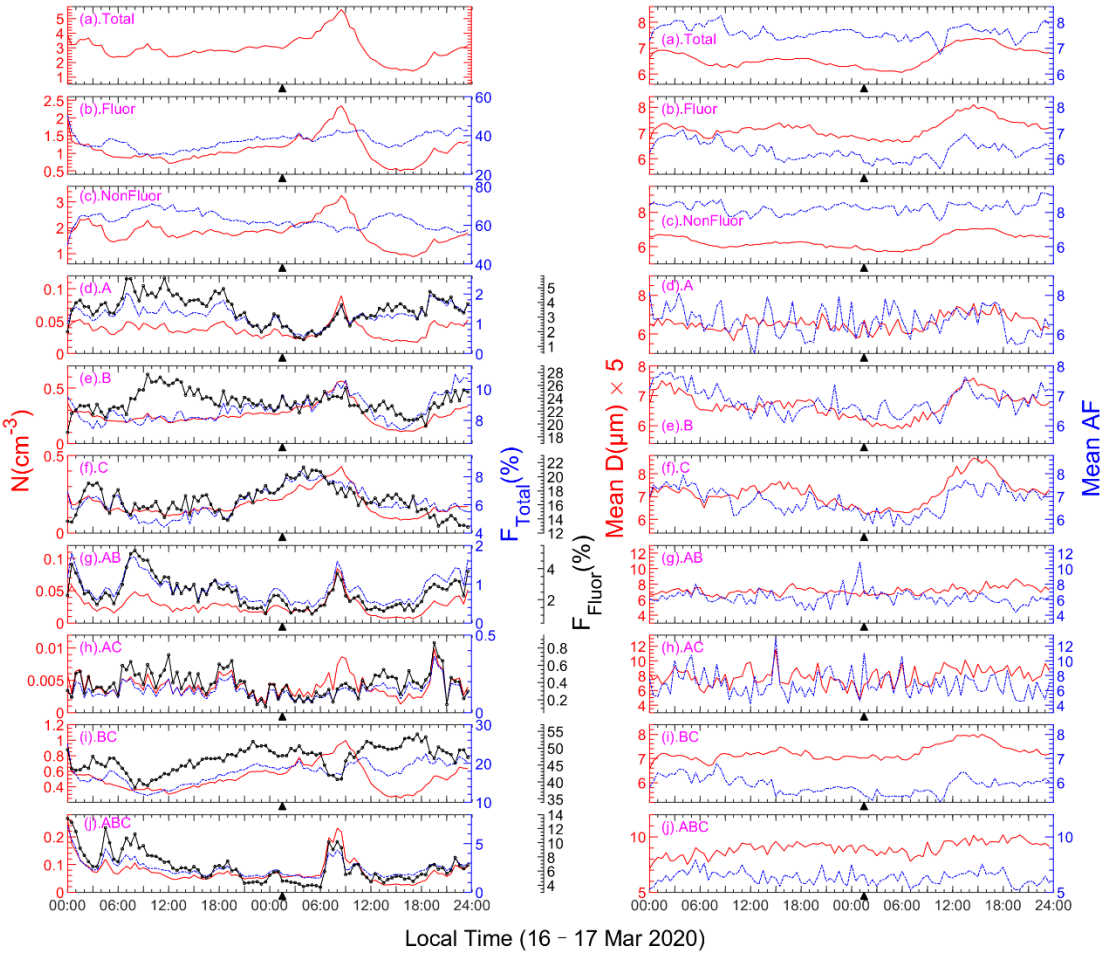

Fig. 5 Left panel: number concentrations (solid red line), number fractions to total particles (blue chain line), and number fractions to fluorescent particles (solid black line with point marker) of investigated particle types. Right panel: Count mean particle diameter (×5, solid red line) and count mean asphericity factor (blue chain line) for investigated particle types measured by WIBS on 16–17 March 2020. The direction of the wind near the surface changes at about 01:30 on 17 March and is marked with a triangle symbol.

”

14. Page 26, Figure 7 (f): Please, use the same vertical scale for PM2.5 (x 10-1) and PM10.

Corrected as suggested.

Changes: line 821-828, Figure 7

“

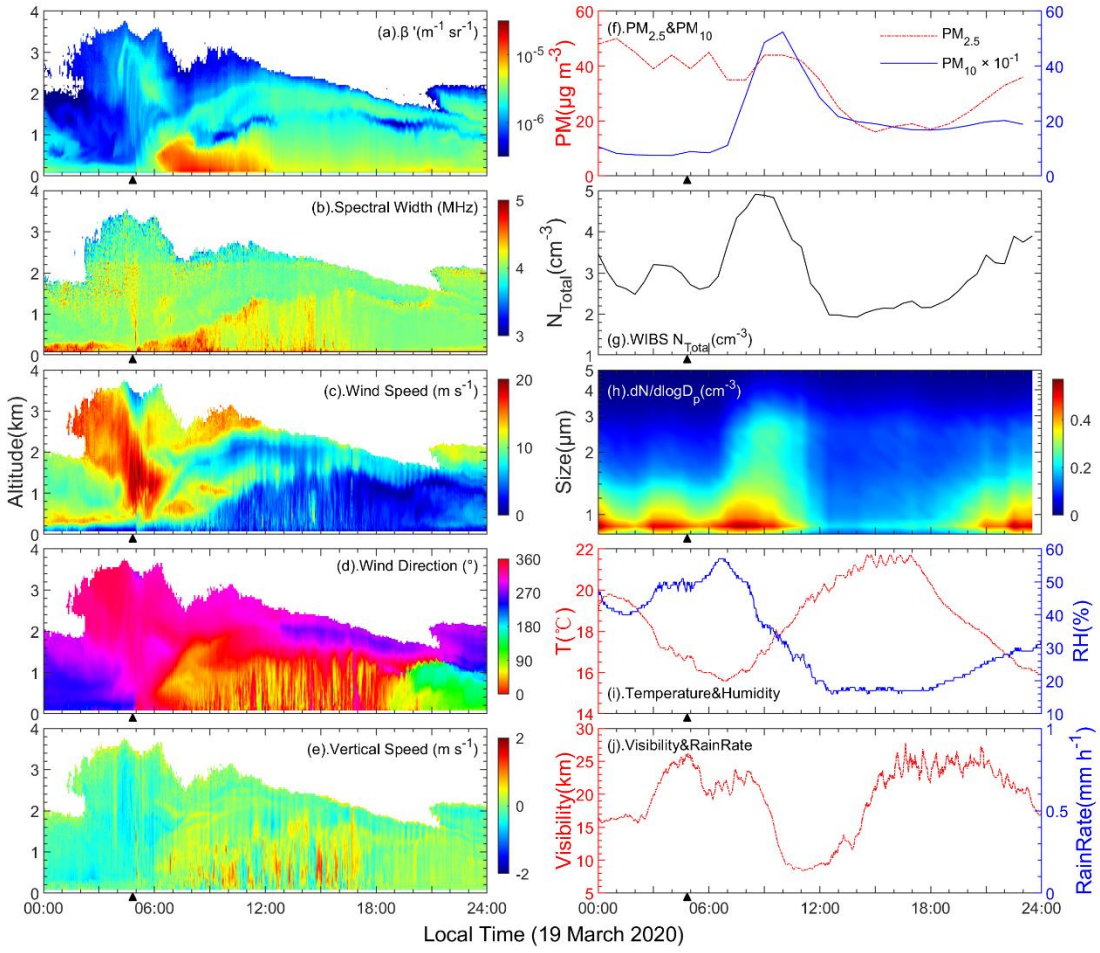

Fig. 7 Left panel: Time-height crosssection of (a) attenuated backscatter coefficient, (b) Doppler spectral width, (c) horizontal wind speed, (d) horizontal wind direction, and (e) vertical wind speed

over Hefei observed by CDWL on 19 March 2020. Right panel: simultaneous ground observation results, including (f) surface hourly particulate matter concentration from local monitor network ($PM_{10}\times10^{-1}$ for readability), (g) number concentration and (h) size distribution of surface total aerosol particles from WIBS, (i) local temperature and humidity, and (j) local visibility and rain rate. The wind direction near the surface changes at about 05:00 on 19 March and is marked with a triangle symbol.

"

15. Page 27, Figure 8 (a)-(j)-right panels: As far as possible, use the same vertical scale for Mean D and Mean AF.

Corrected as suggested.

Changes: line 829-834, figure 8

"

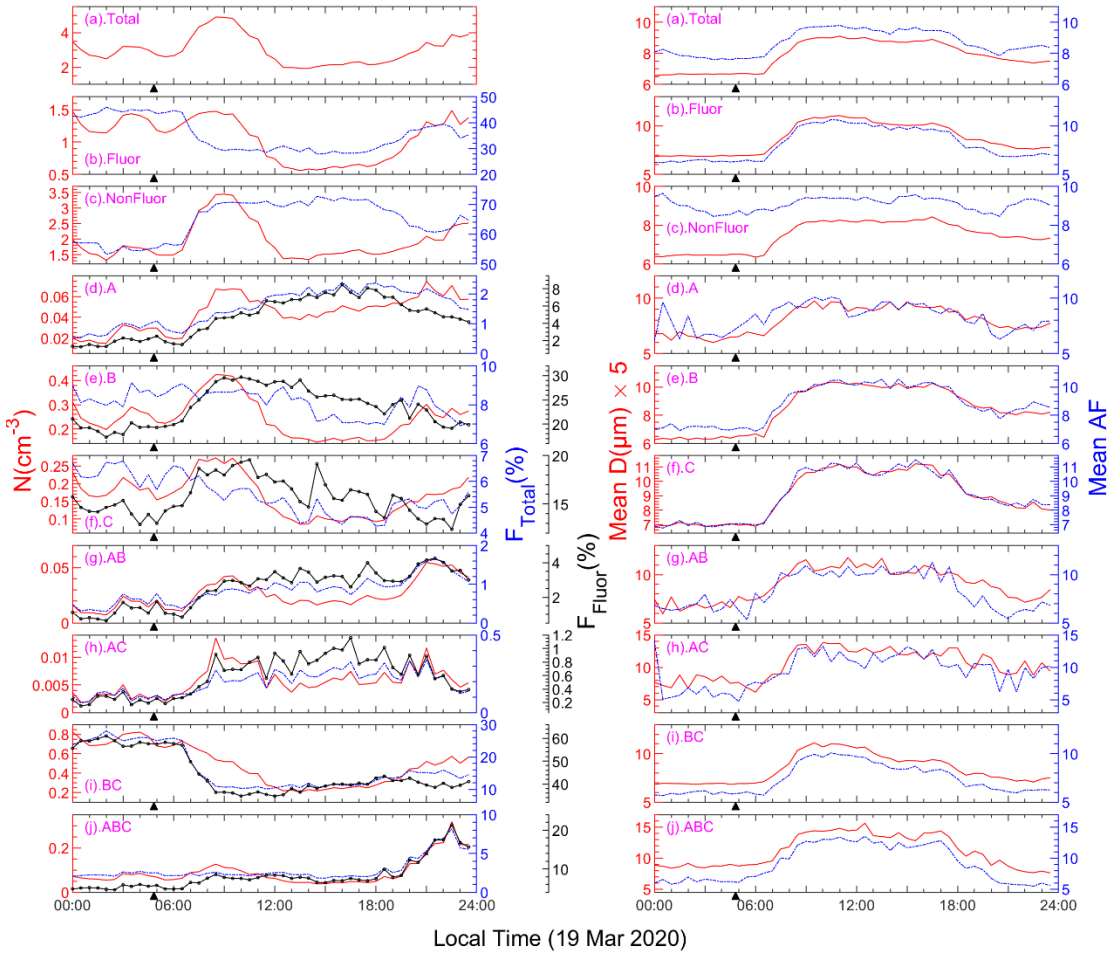

Fig. 8 Left panel: number concentrations (solid red line), number fractions to total particles (blue chain line), and number fractions to fluorescent particles (solid black line with point marker) of investigated particle types. Right panel: Count mean particle diameter (×5, solid red line) and count mean asphericity factor (blue chain line) of investigated particle types measured by WIBS on 19 March 2020. The wind direction near the surface changes at about 05:00 on 19 March and is marked with a triangle symbol.

"

16. In Figures 3, 6 and 9, add more information (web, …) for Natural Earth, where the map data are from.

Additional information of NaturalEarth (naturalearthdata.com) is added in text and capitations of figures.

Changes: line 229-230

"Map data from Natural Earth (naturalearthdata.com) are used to show the HYSPLIT backward trajectory result."

Changes: line 799-800, line 819-820 and line 839-840

"Made with Natural Earth. Free vector and raster map data @ naturalearthdata.com."

References

Chen, Q., Ikemori, F. and Mochida, M.: Light Absorption and Excitation−Emission Fluorescence of Urban Organic Aerosol Components and Their Relationship to Chemical Structure, , doi:10.1021/acs.est.6b02541, 2016.

Chen, Q., Li, J., Hua, X., Jiang, X., Mu, Z., Wang, M., Wang, J., Shan, M., Yang, X., Fan, X., Song, J., Wang, Y., Guan, D. and Du, L.: Identification of species and sources of atmospheric chromophores by fluorescence excitation-emission matrix with parallel factor analysis, Sci. Total Environ., 718, 137322, doi:10.1016/j.scitotenv.2020.137322, 2020.

Crawford, I., Ruske, S., Topping, D. O. and Gallagher, M. W.: Evaluation of hierarchical agglomerative cluster analysis methods for discrimination of primary biological aerosol, Atmos. Meas. Tech., 8(11), 4979–4991, doi:10.5194/amt-8-4979-2015, 2015.

Fröhlich-Nowoisky, J., Kampf, C. J., Weber, B., Huffman, J. A., Pöhlker, C., Andreae, M. O., Lang-Yona, N., Burrows, S. M., Gunthe, S. S., Elbert, W., Su, H., Hoor, P., Thines, E., Hoffmann, T., Després,

V. R. and Pöschl, U.: Bioaerosols in the Earth system: Climate, health, and ecosystem interactions, Atmos. Res., 182, 346–376, doi:10.1016/j.atmosres.2016.07.018, 2016.

Haenel, G., Bullrich, K., Haenel, G. and Bullrich, K.: Physico-chemical property models of tropospheric aerosol particles, BePhA, 51(2), 129–138 [online] Available from: https://ui.adsabs.harvard.edu/abs/1978BePhA..51..129H/abstract (Accessed 8 February 2022), 1978.

Hänel, G.: The Properties of Atmospheric Aerosol Particles as Functions of the Relative Humidity at Thermodynamic Equilibrium with the Surrounding Moist Air, Adv. Geophys., 19(C), 73–188, doi:10.1016/S0065-2687(08)60142-9, 1976.

Hernandez, M., Perring, A. E., McCabe, K., Kok, G., Granger, G. and Baumgardner, D.: Chamber catalogues of optical and fluorescent signatures distinguish bioaerosol classes, Atmos. Meas. Tech., 9(7), 3283–3292, doi:10.5194/amt-9-3283-2016, 2016.

Ho, H. M., Rao, C. Y., Hsu, H. H., Chiu, Y. H., Liu, C. M. and Chao, H. J.: Characteristics and determinants of ambient fungal spores in Hualien, Taiwan, Atmos. Environ., 39(32), 5839–5850, doi:10.1016/j.atmosenv.2005.06.034, 2005.

Hua, N. P., Kobayashi, F., Iwasaka, Y., Shi, G. Y. and Naganuma, T.: Detailed identification of desert-originated bacteria carried by Asian dust storms to Japan, Aerobiologia (Bologna)., 23(4), 291–298, doi:10.1007/s10453-007-9076-9, 2007.

Ichinose, T., Nishikawa, M., Takano, H., Sera, N., Sadakane, K., Mori, I., Yanagisawa, R., Oda, T., Tamura, H., Hiyoshi, K., Quan, H., Tomura, S. and Shibamoto, T.: Pulmonary toxicity induced by intratracheal instillation of Asian yellow dust (Kosa) in mice, Environ. Toxicol. Pharmacol., 20(1), 48–56, doi:10.1016/j.etap.2004.10.009, 2005.

Liu, B., Ichinose, T., He, M., Kobayashi, F., Maki, T., Yoshida, S., Yoshida, Y., Arashidani, K., Takano, H., Nishikawa, M., Sun, G. and Shibamoto, T.: Lung inflammation by fungus, Bjerkandera adusta isolated from Asian sand dust (ASD) aerosol and enhancement of ovalbumin-induced lung eosinophilia by ASD and the fungus in mice, Allergy, Asthma Clin. Immunol., 10(1), 1–12, doi:10.1186/1710-1492-10-10, 2014.

Maki, T., Puspitasari, F., Hara, K., Yamada, M., Kobayashi, F., Hasegawa, H. and Iwasaka, Y.: Variations in the structure of airborne bacterial communities in a downwind area during an Asian dust (Kosa) event, Sci. Total Environ., 488–489(1), 75–84, doi:10.1016/j.scitotenv.2014.04.044, 2014.

Maki, T., Hara, K., Kobayashi, F., Kurosaki, Y., Kakikawa, M., Matsuki, A., Chen, B., Shi, G., Hasegawa, H. and Iwasaka, Y.: Vertical distribution of airborne bacterial communities in an Asian-dust downwind area, Noto Peninsula, Atmos. Environ., 119, 282–293, doi:10.1016/j.atmosenv.2015.08.052, 2015.

Maki, T., Bin, C., Kai, K., Kawai, K., Fujita, K., Ohara, K., Kobayashi, F., Davaanyam, E., Noda, J., Minamoto, Y., Shi, G., Hasegawa, H. and Iwasaka, Y.: Vertical distributions of airborne microorganisms over Asian dust source region of Taklimakan and Gobi Desert, Atmos. Environ., 214(February), 116848, doi:10.1016/j.atmosenv.2019.116848, 2019.

Manninen, A. J., Marke, T., Tuononen, M. and O'Connor, E. J.: Atmospheric Boundary Layer Classification With Doppler Lidar, J. Geophys. Res. Atmos., 123(15), 8172–8189, doi:10.1029/2017JD028169, 2018.

Rodó, X., Ballester, J., Cayan, D., Melish, M. E., Nakamura, Y., Uehara, R. and Burns, J. C.: Association of Kawasaki disease with tropospheric wind patterns, Sci. Rep., 1(March 1986), 1–7, doi:10.1038/srep00152, 2011.

Savage, N., Krentz, C., Könemann, T., Han, T. T., Mainelis, G., Pöhlker, C. and Huffman, J. A.: Systematic Characterization and Fluorescence Threshold Strategies for the Wideband Integrated Bioaerosol Sensor (WIBS) Using Size-Resolved Biological and Interfering Particles, Atmos. Meas. Tech. Discuss., 1–41, doi:10.5194/amt-2017-170, 2017.

Tang, K., Huang, Z., Huang, J., Maki, T., Zhang, S., Shimizu, A., Ma, X., Shi, J., Bi, J., Zhou, T., Wang, G. and Zhang, L.: Characterization of atmospheric bioaerosols along the transport pathway of Asian dust during the Dust-Bioaerosol 2016 Campaign, Atmos. Chem. Phys., 18(10), 7131–7148, doi:10.5194/acp-18-7131-2018, 2018.

Tong, H., Zhang, Y., Filippi, A., Wang, T., Li, C., Liu, F., Leppla, D., Kourtchev, I., Wang, K., Keskinen, H. M., Levula, J. T., Arangio, A. M., Shen, F., Ditas, F., Martin, S. T., Artaxo, P., Godoi, R. H. M., Yamamoto, C. I., De Souza, R. A. F., Huang, R. J., Berkemeier, T., Wang, Y., Su, H., Cheng, Y., Pope, F. D., Fu, P., Yao, M., Pöhlker, C., Petäjä, T., Kulmala, M., Andreae, M. O., Shiraiwa, M., Pöschl, U., Hoffmann, T. and Kalberer, M.: Radical Formation by Fine Particulate Matter Associated with Highly Oxygenated Molecules, Environ. Sci. Technol., 53(21), 12506–12518, doi:10.1021/acs.est.9b05149, 2019.

Wang, C., Jia, M., Xia, H., Wu, Y., Wei, T., Shang, X., Yang, C., Xue, X. and Dou, X.: Relationship analysis of PM2.5 and boundary layer height using an aerosol and turbulence detection lidar, Atmos. Meas. Tech., 12(6), 3303–3315, doi:10.5194/amt-12-3303-2019, 2019.

Wei, T., Xia, H., Yue, B., Wu, Y. and Liu, Q.: Remote sensing of raindrop size distribution using the coherent Doppler lidar, Opt. Express, 29(11), 17246, doi:10.1364/oe.426326, 2021.

Wen, H., Zhou, Y., Xu, X., Wang, T., Chen, Q., Chen, Q., Li, W., Wang, Z., Huang, Z., Zhou, T., Shi, J., Bi, J., Ji, M. and Wang, X.: Water-soluble brown carbon in atmospheric aerosols along the transport pathway of Asian dust: Optical properties, chemical compositions, and potential sources, Sci. Total Environ., 789, 147971, doi:10.1016/j.scitotenv.2021.147971, 2021.

Wu, G., Fu, P., Ram, K., Song, J., Chen, Q., Kawamura, K., Wan, X., Kang, S., Wang, X., Laskin, A. and Cong, Z.: Fluorescence characteristics of water-soluble organic carbon in atmospheric aerosol☆, Environ. Pollut., 268, 115906, doi:10.1016/j.envpol.2020.115906, 2021.

Xu, C., Wei, M., Chen, J., Zhu, C., Li, J., Lv, G., Xu, X., Zheng, L., Sui, G., Li, W., Chen, B., Wang, W., Zhang, Q., Ding, A. and Mellouki, A.: Fungi diversity in PM2.5 and PM1 at the summit of Mt. Tai: Abundance, size distribution, and seasonal variation, Atmos. Chem. Phys., 17(18), 11247–11260, doi:10.5194/acp-17-11247-2017, 2017.

Yu, X., Wang, Z., Zhang, M., Kuhn, U., Xie, Z., Cheng, Y., Pöschl, U. and Su, H.: Ambient measurement of fluorescent aerosol particles with a WIBS in the Yangtze River Delta of China: Potential impacts of combustion-related aerosol particles, Atmos. Chem. Phys., 16(17), 11337–11348, doi:10.5194/acp-16-11337-2016, 2016.

Yue, S., Ren, H., Fan, S., Sun, Y., Wang, Z., Fu, P., Ren, L., Song, T., Li, L., Xie, Q., Li, W., Kang, M., Wei, L., Ren, H., Sun, Y., Wang, Z., Ellam, R. M., Kawamura, K., Fu, P., Academy, C., Sciences, A. and Sciences, E.: Springtime precipitation effects on the abundance of fluorescent biological aerosol particles and HULIS in Beijing, Sci. Rep., 6(1), 29618, doi:10.1038/srep29618, 2016.

Yue, S., Ren, L., Song, T., Li, L., Xie, Q., Li, W., Kang, M., Zhao, W., Wei, L., Ren, H., Sun, Y., Wang, Z., Ellam, R. M., Liu, C. Q., Kawamura, K. and Fu, P.: Abundance and Diurnal Trends of Fluorescent Bioaerosols in the Troposphere over Mt. Tai, China, in Spring, J. Geophys. Res. Atmos., 124(7), 4158–4173, doi:10.1029/2018JD029486, 2019.